Assimilation of autoscaled data and regional and local ionospheric models as input source for a real-time 3-D IRI modeling

M. Pezzopane[1], M. Pietrella[1], A. Pignatelli[1], B. Zolesi[1], Lj. R. Cander[2]

[1]Istituto Nazionale di Geofisica e Vulcanologia, Via di Vigna Murata 605, 00143, Rome, Italy

[2]Rutherford Appleton Laboratory, Didcot, OX11 0QX, UK

Correspondence to: M. Pezzopane (michael.pezzopane@ingv.it)

Abstract

This paper describes how the joint utilization of autoscaled data such as the F2 peak critical frequency *fo*F2, the propagation factor *M*(3000)F2 and the electron density profile, coming from two reference ionospheric stations (Rome and Gibilmanna), the regional (SIRMUP) and global (IRI) ionospheric models, can provide a valid tool for obtaining a real-time three-dimensional (3-D) electron density mapping of the ionosphere. Preliminary results of the proposed 3-D model are shown by comparing the electron density profiles given by the model with the ones measured at three testing ionospheric stations (Athens, Roquetes and S.Vito).

Keywords: Ionosphere; Electron Density; Ionogram; IRI; Modeling

1. Introduction

Ionospheric models are important for many research, engineering and educational purposes in providing comprehensive specification of the three-dimensional (3-D) electron density profile [*Bilitza*, 2002; *Sojka et al*., 2006; *Cander*, 2008; *Eccles et al*., 2011 and references therein]. Most of them are global, e.g. the International Reference Ionosphere (IRI) [*Bilitza and Reinisch*, 2008] and the NeQuick [*Radicella*, 2009], in which for a particular location the separate input ionospheric characteristics are modeled as a function of latitude, longitude, time-of-day, season and epoch of the solar cycle. The basic input data to the ionospheric models come from past and/or current worldwide network of vertical-sounding or topside measurements and satellite observations, from profound theoretical considerations and from various combinations of these. Although global models of the F2 layer critical frequency *fo*F2 and propagation factor *M*(3000)F2, such as the CCIR [1991] and the URSI [*Rush et al*., 1989], represent a valid input source for a 3-D modeling of the ionosphere, regional and local models of these ionospheric characteristics can be important complements to characterize those features that may be easily neglected in global models. They are also good validation tools for global models and should be considered as a significant part of any ionospheric modeling efforts. It is important to mention here that the ionosphere related European COST (COoperation in Scientific and Technology) actions [*Bradley*, 1995; *Hanbaba*, 1999] have clearly demonstrated that regional *fo*F2 and *M*(3000)F2 models can give better results than global models of these ionospheric characteristics. This is particularly valid for nowcasting models that perform better than long-term prediction models, especially during disturbed conditions [*Pietrella et al*., 2009].

Modern real-time ionosonde observations provide an extremely valuable data source for addressing different scientific and application issues related to ionospheric modeling. Based on these data, much progress has been made in recent years in constructing empirical regional and local models of *fo*F2 and

M(3000)F2 ionospheric characteristics. One of them is the real-time Simplified Ionospheric Regional Model UPdated (SIRMUP) [*Zolesi et al*., 2004; *Tsagouri et al*., 2005], which has been successfully operating in the European area within the framework of the DIAS project [*Belehaki et al*., 2006]. The SIRMUP procedure is based on the idea that real-time values of *fo*F2 at one location can be determined from the Simplified Ionospheric Regional Model (SIRM) [*Zolesi et al*., 1996] by using an effective sunspot number (R_{eff}), based on real-time ionosonde observations, instead of the smoothed sunspot number R_{12}. The method of determining R_{eff} was introduced and described in details by *Houminer et al*. [1993]. R_{eff} is chosen to give the best fit between model calculation and real measurements obtained from a grid of ionosondes located in the mapping area. The SIRMUP has the capability to generate the real-time updated *fo*F2 and *M*(3000)F2 values on a user specified spatial grid. Area coverage can be regional, over a few ionospheric stations, or local over only one station.

In this paper it will be shown how a combined utilization of the real-time autoscaled *fo*F2 and *M*(3000)F2 data as well as the real-time electron density profiles coming from the reference ionospheric stations of Rome (41.8°N, 12.5°E) and Gibilmanna (37.9°N, 14.0°E) and the SIRMUP model can provide a valid tool for improving real-time 3-D electron density modeling by IRI. The new approach is used to estimate the electron density on a regional grid of the ionosphere in the Central Mediterranean area extended in latitude from 30° to 44° and in longitude from -5° to 40° with a 1° x 1° degree resolution. The proposed 3-D model is presented and validated by comparing the corresponding electron density profiles with those directly measured at the three testing ionospheric stations: Athens (38.0°N, 23.5°E), Roquetes (40.8°N, 0.5°E) and S.Vito (40.6°N, 17.8°E).

2. Description of the proposed 3-D electron density model of the ionosphere

Under the assumption of space-sparse ionospheric measurements, data assimilation is the process of merging measurement data with a model to estimate the ionospheric conditions over an area where direct measurements are not available. By means of data assimilation, it is possible to expand the effectiveness of limited measurements by using the model and, at the same time, increase the accuracy of model estimates using the measurements. For this reason, in the last decade much work has been performed to develop and continuously test models that after assimilating observations compute an updated 3-D image of the ionosphere. The Electron Density Assimilative Model (EDAM) [*Angling and Khattatov*, 2006], developed by QinetiQ, uses slant total electron content (TEC) GPS ground-based measurements to adjust an empirical 3-D climatological distribution of the ionospheric electron density. The Utah State University Global Assimilation of Ionospheric Model (GAIM) [*Schunk et al*., 2004] can assimilate both slant TEC GPS ground-based observations and ionosonde electron density profiles using a Gauss-Markov technique, and it has been continuously tested and improved [*Thompson et al*., 2006; *Decker and McNamara*, 2007; *McNamara et al*., 2007, 2008, 2010, 2011]. In our case data assimilation is performed with the autoscaled *fo*F2 and *M*(3000)F2 values and the autoscaled electron density profiles.

Figure 1 shows the flowchart of the algorithm for the 3-D electron density model of the ionosphere described in this paper. The initial step of the algorithm consists in considering the autoscaling performed at some ionospheric stations. In our study, the autoscaling performed by Autoscala [*Pezzopane and Scotto*, 2005, 2007] on the ionograms recorded by the AIS-INGV ionosonde [*Zuccheretti et al*., 2003] installed at the ionospheric stations of Rome (41.8°N, 12.5°E) and Gibilmanna (37.9°N, 14.0°E) is exploited. The quality of the autoscaled ionograms computed by Autoscala is not checked as for instance QualScan [*McNamara*, 2006] does for the autoscaled

ionograms computed by ARTIST before assimilating them into GAIM. However, it is noteworthy to point out that during recent years several routines were developed to considerably increase the reliability and accuracy of Autoscala [*Scotto and Pezzopane*, 2008; *Pezzopane and Scotto*, 2010].

If no station has given as output the autoscaled values of *fo*F2 and *M*(3000)F2, the standard IRI-URSI procedure is launched and a 3-D climatological matrix (from now on called IRI-URSI) of the electron density is generated.

However, if at least one station has given as output the real-time autoscaled values of the critical frequency *fo*F2 and the propagation factor *M*(3000)F2, the R_{eff} is calculated on the basis of these values [*Zolesi et al*., 2004; *Tsagouri et al*., 2005] and it is then used by the SIRM model [*Zolesi et al*., 1996] to provide a nowcasting of *fo*F2 and *M*(3000)F2 on a spatial grid that can be regional or local. In the next step, this *fo*F2 and *M*(3000)F2 grid of values produced by the SIRMUP procedure is used as input to the IRI and a 3-D updated matrix of the electron density is generated (from now on called IRI-SIRMUP). At this stage, if no station has an electron density profile associated to the performed autoscaling, the process stops. On the other hand, if at least one ionospheric station has an electron density profile associated to the performed autoscaling, an assimilation process of the measured electron density profiles (see the next section) starts: the IRI-SIRMUP electron densities are updated at a specific height *h*, and a further updated 3-D matrix (from now on called IRI-SIRMUP-P) of the electron density profile is generated. As in certain cases Autoscala outputs only the ionospheric characteristics without producing an electron density profile, it is important to underline the necessity to check whether a station has provided an electron density profile, even though it has already given *fo*F2 and *M*(3000)F2 autoscaled values. For instance, when the ionogram trace is almost totally blanketed by a strong E sporadic layer except for the last part of the F2 layer trace, Autoscala identifies this asymptotical ending trace of the F2 layer, giving as output *fo*F2 and *M*(3000)F2. However, under

such circumstances these values alone could not be sufficient to produce a realistic electron density profile.

2.1 *Assimilation process of the measured electron density profiles*

In order to assimilate the measured electron density profiles obtained by the autoscaling inversion of the ionograms recorded at the reference ionospheric stations of Rome and Gibilmanna [*Scotto*, 2009], the following interpolation process between the measured electron density values and those calculated by the IRI-SIRMUP procedure is applied.

Given a definite height *h*,

$$\{x_1(\lambda_1, \vartheta_1), x_2(\lambda_2, \vartheta_2), ...x_i(\lambda_i, \vartheta_i), ...x_n(\lambda_n, \vartheta_n)\} \quad (1)$$

represent the geographical points (with i=1,….,n, and where λ and θ are the corresponding geographical longitude and latitude) for which the modeled IRI-SIRMUP values I of the electron density

$$\{I[x_1(\lambda_1, \vartheta_1)], I[x_2(\lambda_2, \vartheta_2)], ...I[x_i(\lambda_i, \vartheta_i)], ...I[x_n(\lambda_n, \vartheta_n)]\} \quad (2)$$

are known.

On the other hand,

$$\left\{\overline{x_{1*}}(\lambda_{1*}, \vartheta_{1*}), \overline{x_{2*}}(\lambda_{2*}, \vartheta_{2*}), ...\overline{x_j}(\lambda_j, \vartheta_j), ...\overline{x_m}(\lambda_m, \vartheta_m)\right\} \quad (3)$$

represent the points (with j=1*,….,m) for which the measured values M of the electron density

$$\left\{M[\overline{x_{1*}}(\lambda_{1*},\vartheta_{1*})], M[\overline{x_{2*}}(\lambda_{2*},\vartheta_{2*})],....., M[\overline{x_j}(\lambda_j,\vartheta_j)],....M[\overline{x_m}(\lambda_m,\vartheta_m)]\right\} \quad (4)$$

are known (in our case m=2).

The distance

$$d_{ij} = x_i(\lambda_i,\vartheta_i) - \overline{x_j}(\lambda_j,\vartheta_j) \quad (5)$$

is then defined.

Hence, for each point for which a measured value of the electron density is available close by, a weight function

$$G_{ij} = G(d_{ij}) = \exp\left(-\frac{d_{ij}^{\,2}}{2\sigma^2}\right) \quad (6)$$

can be defined. The weight function is then equal to 1 at the point where the measured value of the electron density is available and it decays as d_{ij} increases. Figure 2 shows the effect of the weight function for two different values of σ, the larger is the value of σ, the larger is the area affected by the measured values. Given a generic point x_i, the corresponding value T of the electron density is calculated on the basis of the weight function and of the measured electron density profiles obtained by Autoscala as follows

$$T[x_i(\lambda_i,\vartheta_i)] = \sum_{j=1}^{m}\left\{G_{ij}M[\overline{x_j}(\lambda_j,\vartheta_j)] + \left[1-G_{ij}\right]I[x_i(\lambda_i,\vartheta_i)]\right\}. \quad (7)$$

In order to show the differences between the 3-D matrixes IRI-URSI and IRI-SIRMUP-P, corresponding Figures 3, 4, and 5 illustrate horizontal slices, at a fixed height, and vertical slices, at a fixed latitude and at a fixed longitude, of the electron density over the Central Mediterranean area under consideration extracted from each of these matrixes for the 16 February 2010 at 07:00 UT. In particular, with regard to the IRI-SIRMUP-P matrix, different maps for different value of σ are shown. Figures 3, 4, and 5 highlight clearly how in general the differences between climatological models (in this case the IRI-URSI) and models that assimilate measured values may be remarkable. Moreover, with regard to the IRI-SIRMUP-P matrixes it is evident that the larger is the value of σ, the larger is the area affected by the measured values. On the contrary, the lower is the value of σ, the smaller is the area affected by the measured values. In this latter case, if the measured values are pretty different from the values of the IRI-SIRMUP matrix, distinct patches characterize the IRI-SIRMUP-P matrix as it is visible for instance in Figure 4b at a longitude of 14°E (corresponding to the location of Gibilmanna) between about 170 and 220 km of altitude.

In order to compute Figures 3-5, the simple Matlab “contourc” function was used, that is merely a graphical linear interpolation between the edges of the squares of the grid (further information on this Matlab function can be found at the site http://www.mathworks.com/help/techdoc/creating_plots/f10-2524.html#f10-2614).

3. Preliminary validation results

Preliminary validation results of the proposed IRI-SIRMUP-P 3-D model are here shown by comparing the electron density profiles given by the model with the ones measured at some testing ionospheric stations. As shown in Figure 6, the reference ionospheric stations considered as input for

the model are Rome and Gibilmanna, while the ionospheric stations considered as test sites are Roquetes, S. Vito and Athens.

The data and the electron density profiles measured at Rome and Gibilmanna are those autoscaled by Autoscala from the ionograms recorded by the AIS-INGV ionosonde, while the data and the electron density profiles measured at Roquetes, S. Vito and Athens are those autoscaled by ARTIST [*Reinisch and Huang*, 1983; *Reinisch et al*., 2005; *Galkin and Reinisch*, 2008] from the ionograms recorded by the DPS4 digisonde [*Bibl and Reinisch*, 1978]. The release of ARTIST installed at Roquetes and S. Vito is the 4.0, while the one installed at Athens is the 4.5.

In order to test the model for quasi-stationary ionospheric conditions and at the solar terminator, the two geomagnetically quiet days 28 September 2009 from 11:15 to 13:45 UT (Kp=2) and 16 February 2010 from 06:00 to 08:45 UT (Kp=2) were selected. Both periods were particularly appropriate to test the model because both the autoscaling performed by ARTIST at Roquetes, S. Vito and Athens, and the autoscaling performed by Autoscala at Rome and Gibilmanna were available. The results of the test are shown from Figure 7 to Figure 12 where the electron density profiles obtained by the IRI-URSI procedure, by the IRI-SIRMUP-P procedure, and by the ARTIST system are compared. The IRI-URSI profiles were calculated till to a maximum height of 500 km, while the maximum height of the IRI-SIRMUP-P profiles is equal to 400 km because Autoscala models the topside as a parabolic layer ending right at that height. The matrix IRI-SIRMUP-P from which the corresponding profile at the test site is extracted was calculated by setting σ=3.0. This choice of σ follows a preliminary testing phase (not shown here) of the model for different values of σ where the best results were obtained for σ=3.0.

Figures 7-9 show that for quasi-stationary ionospheric conditions the electron density profile extracted from the IRI-URSI and from the IRI-SIRMUP-P matrixes are pretty similar, mostly from 12:15 to 13:45 UT, and that both of them are in good agreement with the electron density profile

measured by ARTIST. This represents a further evidence that the IRI can satisfactorily model an undisturbed and stationary ionosphere.

Figures 10-12 show that at the solar terminator the electron density profile extracted from the IRI-SIRMUP-P matrix is more representative of the real conditions of the ionosphere than the electron density profile extracted from the IRI-URSI matrix. Obviously, the best results were obtained for S. Vito that is the test site closest to the input sites of Rome and Gibilmanna. Focusing our attention on the first plot of Figure 12, we can see that this is the only case for which the IRI-SIRMUP-P profile underestimates the measured one given as output by ARTIST. In order to understand this, the autoscaling performed by Autoscala at the ionogram recorded at Gibilmanna on 16 February 2010 at 06:00 UT is shown in Figure 13. The ionogram quality is not so good, the trace is a little truncated and consequently the trace identified by Autoscala underestimates the real one. This underestimation made by Autoscala, due to the assimilation process of the measured electron density profile described in the section 2.1, affects the IRI-SIRMUP-P profile computed at S. Vito. It is worth mentioning here that in general the ionograms recorded at Rome and Gibilmanna by the AIS-INGV ionosonde are of high-quality and that the reliability of Autoscala is proven good [*Pezzopane and Scotto*, 2007, 2008]. On the contrary, focusing our attention on the first plots of Figures 10 and 11, we can see that the IRI-SIRMUP-P profile overestimates the measured one given as output by ARTIST. The reason of this overestimation is probably due to the lack of ionospheric stations closer to Athens and Roquetes than Rome and Gibilmanna, which might provide real-time electron density profiles to be used as input for the IRI-SIRMUP-P model and consequently help the model in better representing the real conditions of the ionosphere.

Figures 14 and 15 illustrate additional results in terms of the differences ($foF2_{ARTIST-DPS4}$-$foF2_{IRI-SIRMUP-P[sigma=3.0]}$) and ($foF2_{ARTIST-DPS4}$-$foF2_{IRI-URSI}$) of the critical frequency *fo*F2 values obtained at

Athens, Roquetes and S. Vito by the IRI-URSI procedure, by the IRI-SIRMUP-P procedure (with σ=3.0), and by the ARTIST system. They confirm both previous conclusions that the IRI-SIRMUP-P procedure is more representative of the real ionospheric conditions than the standard IRI-URSI procedure, and that the best results are obtained for the S. Vito test site.

4. Conclusions

In this paper we have proposed a model for which updated values of *fo*F2 and *M*(3000)F2, coming from the regional ionospheric nowcasting model SIRMUP, plus the entire electron density profiles coming from the autoscaled inversion of the ionograms recorded at the reference stations of Rome and Gibilmanna, are used as input data for IRI to provide a real-time 3-D matrix of the electron density. We have also shown some preliminary results illustrating how this approach can give a real improvement to the regional 3-D picture of the ionosphere. Further additional tests are planned on geomagnetically disturbed periods by means of more than two reference ionospheric stations providing real-time data as input for the model. It will also be interesting to apply the proposed 3-D model on other global models such as for instance the NeQuick model [*Radicella*, 2009].

Acknowledgements

The authors gratefully acknowledge the three reviewers for their helpful comments and suggestions.

References

Angling, M. J., and B. Khattatov (2006), Comparative study of two assimilative models of the ionosphere, *Radio Sci*., 41, RS5S20, doi:10.1029/2005RS003372.

Belehaki, A., Lj. R. Cander, B. Zolesi, J. Bremer, C. Juren, I. Stanislawska, D. Dialetis, and M. Hatzopoulos (2006), Monitoring and Forecasting the Ionosphere Over Europe: The DIAS Project, *Space Weather J*., 4(12), S12002, doi:10.1029/2006SW000270.

Bibl., K., and B. W. Reinisch (1978), The universal digital ionosonde, *Radio Sci*., 13(3), doi:10.1029/RS013i003p00519.

Bilitza, D. (2002), Ionospheric models for radio propagation studies, in *Review of Radio Sci*. 1999-2002, pp. 625-680, Ed. W. Ross Stone, John Wiley&Sons, New York, USA.

Bilitza, D., and B. W. Reinisch (2008), International Reference Ionosphere 2007: Improvements and new parameters, *Adv*. *Space Res*., 42(4), 599-609, doi:10.1016/j.asr.2007.07.048.

Bradley, P. A. (1995), PRIME (Prediction Regional Ionospheric Modeling over Europe), *COST Action 238 Final Report*, Commission of the European Communities, Brussels, Belgium.

Cander, Lj. R. (2008), Ionospheric research and space weather services, *J*. *Atmos*. *Sol*. *Terr*. *Phys*., 70(15), 1870–1878, doi:10.1016/j.jastp.2008.05.010.

Comité Consultatif International des Radiocommunications (CCIR) (1991), Atlas of ionospheric characteristics, *Report 340-6*, Geneva, Switzerland.

Decker, D. T., and L. F. McNamara (2007), Validation of ionospheric weather predicted by Global Assimilation of Ionospheric Measurements (GAIM) models, *Radio Sci*., 42, RS4017, doi:10.1029/2007RS003632.

Eccles, V., J. Thompson, J. J. Sojka, H. Vo, and S. Gonzalez (2011), Assessment of Ionospheric Models package for the Community Coordinated Modeling Center: Climatology, *Space Weather J*., 9, S01004, doi:10.1029/2010SW000596.

Galkin, I. A., and B. W. Reinisch (2008), The new ARTIST 5 for all digisondes, *Ionosonde Network Advisory Group Bulletin* 69, 8pp., URL: http://www.ips.gov.au/ IPSHosted/INAG/web-69/2008/artist5-inag.pdf.

Hanbaba, R. (1999), Improved Quality of Service in Ionospheric Telecommunication Systems Planning and Operation, *COST Action 251 Final Report*, Space Research Centre, Warsaw, Poland.

Houminer, Z., J. A. Bennett, and P. L. Dyson (1993), Real-time ionospheric model updating, *J. Electr. Electron. Eng*., 13(2), 99–104.

McNamara, L. F. (2006), Quality figures and error bars for autoscaled Digisonde vertical incidence ionograms, *Radio Sci*., 41, RS4011, doi:10.1029/2005RS003440.

McNamara, L. F., C. R. Baker, and D. T. Decker (2008), Accuracy of USU-GAIM specifications of foF2 and M(3000)F2 for a worldwide distribution of ionosonde locations, *Radio Sci*., 43, RS1011, doi:10.1029/2007RS003754.

McNamara, L. F., G. J. Bishop, and J. A. Welsh (2011), Assimilation of ionosonde profiles into a global ionospheric model, *Radio Sci*., doi:10.1029/2010RS004457.

McNamara, L. F., D. T. Decker, J. A. Welsh, and D. G. Cole (2007), Validation of the Utah State University Global Assimilation of Ionospheric Measurements (GAIM) model predictions of the maximum usable frequency for a 3000 km circuit, *Radio Sci*., 42, RS3015, doi:10.1029/2006RS003589.

McNamara, L. F., J. M. Retterer, C. R. Baker, G. J. Bishop, D. L. Cooke, C. J. Roth, and J. A. Welsh (2010), Longitudinal structure in the CHAMP electron densities and their implications for global ionospheric modeling, *Radio Sci*., 45, RS2001, doi:10.1029/2009RS004251.

Pezzopane, M., and C. Scotto (2005), The INGV software for the automatic scaling of foF2 and MUF(3000)F2 from ionograms: a performance comparison with ARTIST 4.01 from Rome data, *J. Atmos. Sol. Terr. Phys*., 67(12), 1063-1073, doi:10.1016/j.jastp.2005.02.022.

Pezzopane, M., and C. Scotto (2007), The Automatic Scaling of Critical Frequency foF2 and MUF(3000)F2: a comparison between Autoscala and ARTIS 4.5 on Rome data, *Radio Sci*. 42, RS4003, doi:10.1029/2006RS003581.

Pezzopane, M., and C. Scotto (2008), A method for automatic scaling of F1 critical frequencies from ionograms, *Radio Sci*. 43, RS2S91, doi:10.1029/2007RS003723.

Pezzopane, M., and C. Scotto (2010), Highlighting the F2 trace on an ionogram to improve Autoscala performance, *Comp*. *Geosc*., 36, 1168-1177, doi:10.1016/j.cageo.2010.01.010.

Pietrella , M., L. Perrone, G. Fontana, V. Romano, A. Malagnini, G. Tutone, B. Zolesi, Lj. R. Cander, A. Belehaki, I. Tsagouri, S. S. Kouris, F. Vallianatos, J. P. Makris, and M. J. Angling (2009), Oblique-incidence ionospheric soundings over Central Europe and their application for testing now casting and long term prediction models, *Adv*. *Space Res*., 43(11), 1611-1620, doi:10.1016/j.asr.2008.01.022.

Radicella, S. M. (2009), The NeQuick model genesis, uses and evolution, *Ann*. *Geophys*. *Italy*, 52(3/4), 417-422.

Reinisch, B.W., and X. Huang (1983), Automatic calculation of electron density profiles from digital ionograms 3. Processing of bottom side ionograms, *Radio Sci*., 18(3), doi:10.1029/RS018i003p00477.

Reinisch, B. W., X. Huang, I. A. Galkin, V. Paznukhov, and A. Kozlov (2005), Recent advances in real-time analysis of ionograms and ionospheric drift measurements with digisondes, *J. Atmos. Sol. Terr. Phys.*, 67(12), 1054–1062, doi:10.1016/j.jastp.2005.01.009.

Rush C., M. Fox, D. Bilitza, K. Davies, L. McNamara, F. Stewart, and M. PoKempner (1989), Ionospheric Mapping: An Update of foF2 Coefficients, *Telecommunication J.*, 56, 179-182.

Schunk, R. W., L. Scherliess, J. J. Sojka, D. C. Thompson, D. N. Anderson, M. Codrescu, C. Minter, T. J. Fuller-Rowell, R. A. Heelis, M. Hairston, and B. M. Howe. (2004), Global Assimilation of Ionospheric Measurements (GAIM). *Radio Sci.*, RS1S02, doi:10.1029/2002RS002794.

Scotto, C. (2009), Electron density profile calculation technique for Autoscala ionogram analysis, *Adv. Space Res.*, 44(6), 756-766, doi:10.1016/j.asr.2009.04.037.

Scotto, C, and M. Pezzopane (2008), Removing multiple reflections from the F2 layer to improve Autoscala performance, *J. Atmos. Sol. Terr. Phys.*, 70(15), 1929-1934, doi:10.1016/j.jastp.2008.05.012.

Sojka, J. J., C. Smithtro, and R. W. Schunk (2006), Recent developments in ionosphere–thermosphere modeling with an emphasis on solar-variability, *Adv. Space Res.*, 37(2), 369–379, doi:10.1016/j.asr.2005.10.032.

Thompson, D. C., L. Scherliess, J. J. Sojka, and R. W. Schunk, (2006), The Utah State University Gauss-Markov Kalman filter of the ionosphere: the effect of slant TEC and electron density profile data on model fidelity, *J. Atmos. Sol. Terr. Phys.*, 68(9), 947-958, doi:10.1016/j.jastp.2005.10.011.

Tsagouri, I, B. Zolesi, A. Belehaki, and Lj. R. Cander (2005), Evaluation of the performance of the real-time updated simplified ionospheric regional model for the European area, *J. Atmos. Sol. Terr. Phys.*, 67(12), 1137-1146, doi:10.1016/j.jastp.2005.01.012.

Zolesi, B., L. R. Cander, and G. de Franceschi (1996), On the potential applicability of the Simplified Ionospheric Regional Model to different midlatitude areas, *Radio Sci.*, 31(3), 547–552.

Zolesi, B., A. Belehaki, I. Tsagouri, and Lj. R. Cander (2004), Real-time updating of the simplified ionospheric regional model for operational applications, *Radio Sci.*, 39, RS2011, doi:10.1029/2003RS002936.

Zuccheretti, E., G. Tutone, U. Sciacca, C. Bianchi, and B. J. Arokiasamy (2003), The new AIS-INGV digital ionosonde, *Ann. Geophys. Italy*, 46(4), 647–659.

Figure 1. Flowchart showing the algorithm of the 3-D electron density model of the ionosphere described in this paper.

Figure 2. Effect of the weight function on the area under consideration for two different values of σ.

Figure 3. Maps of the electron density (electrons/cm^3) at fixed height 210 km obtained by (a) IRI-URSI, and IRI-SIRMUP-P with (b) σ=0.5, (c) σ=1.0, (d) σ=3.0, (e) σ=5.0, and (f) σ=7.0.

Figure 4. Maps of the electron density (electrons/cm^3) at fixed latitude 38°N obtained by (a) IRI-URSI, and IRI-SIRMUP-P with (b) σ=0.5, (c) σ=1.0, (d) σ=3.0, (e) σ=5.0, and (f) σ=7.0.

Figure 5. Maps of the electron density (electrons/cm^3) at fixed longitude 14°E obtained by (a) IRI-URSI, and IRI-SIRMUP-P with (b) σ=0.5, (c) σ=1.0, (d) σ=3.0, (e) σ=5.0, and (f) σ=7.0.

Figure 6. Map of the Central Mediterranean area under study. Red stars represent the ionospheric stations considered as input for the model. Blue stars represent the ionospheric stations considered as test sites.

Figure 7. Comparison among the profiles obtained at Athens on 28 September 2009 from 11:15 to 13:45 UT by IRI-SIRMUP-P with σ=3.0 (in green), ARTIST (in red), and IRI-URSI (in blue).

Figure 8. Comparison among the profiles obtained at Roquetes on 28 September 2009 from 11:15 to 13:45 UT by IRI-SIRMUP-P with σ=3.0 (in green), ARTIST (in red), and IRI-URSI (in blue).

Figure 9. Comparison among the profiles obtained at S. Vito on 28 September 2009 from 11:15 to 13:45 UT by IRI-SIRMUP-P with σ=3.0 (in green), ARTIST (in red), and IRI-URSI (in blue).

Figure 10. Comparison among the profiles obtained at Athens on 16 February 2010 from 06:00 to 08:45 UT by IRI-SIRMUP-P with σ=3.0 (in green), ARTIST (in red), and IRI-URSI (in blue).

Figure 11. Comparison among the profiles obtained at Roquetes on 16 February 2010 from 06:00 to 08:45 UT by IRI-SIRMUP-P with σ=3.0 (in green), ARTIST (in red), and IRI-URSI (in blue).

Figure 12. Comparison among the profiles obtained at S. Vito on 16 February 2010 from 06:00 to 08:45 UT by IRI-SIRMUP-P with σ=3.0 (in green), ARTIST (in red), and IRI-URSI (in blue).

Figure 13. (a) Ionogram recorded at Gibimanna by the AIS-INGV ionosonde on 16 February at 06:00 UT and (b) autoscaled by Autoscala. In red the ordinary trace identified by Autoscala and in green the corresponding electron density profile. Table "AIP output" shows the parameters used by Autoscala to estimate the electron density profile associated with the reconstructed ordinary trace.

Figure 14. Comparison between the differences ($foF2_{\text{ARTIST-DPS4}}$-$foF2_{\text{IRI-SIRMUP-P[sigma=3.0]}}$) (in green) and ($foF2_{\text{ARTIST-DPS4}}$-$foF2_{\text{IRI-URSI}}$) (in blue) of the critical frequency *fo*F2 values obtained at (a) Athens, (b) Roquetes, and (c) S. Vito by IRI-URSI, IRI-SIRMUP-P with σ=3.0, and ARTIST on 28 September 2009 from 11:15 to 13:45 UT.

Figure 15. Comparison between the differences ($fo\mathrm{F2}_{\mathrm{ARTIST\text{-}DPS4}}$-$fo\mathrm{F2}_{\mathrm{IRI\text{-}SIRMUP\text{-}P[sigma=3.0]}}$) (in green) and ($fo\mathrm{F2}_{\mathrm{ARTIST\text{-}DPS4}}$-$fo\mathrm{F2}_{\mathrm{IRI\text{-}URSI}}$) (in blue) of the critical frequency *fo*F2 values obtained at (a) Athens, (b) Roquetes, and (c) S. Vito by IRI-URSI, IRI-SIRMUP-P with σ=3.0, and ARTIST on 16 February 2010 from 06:00 to 08:45 UT.

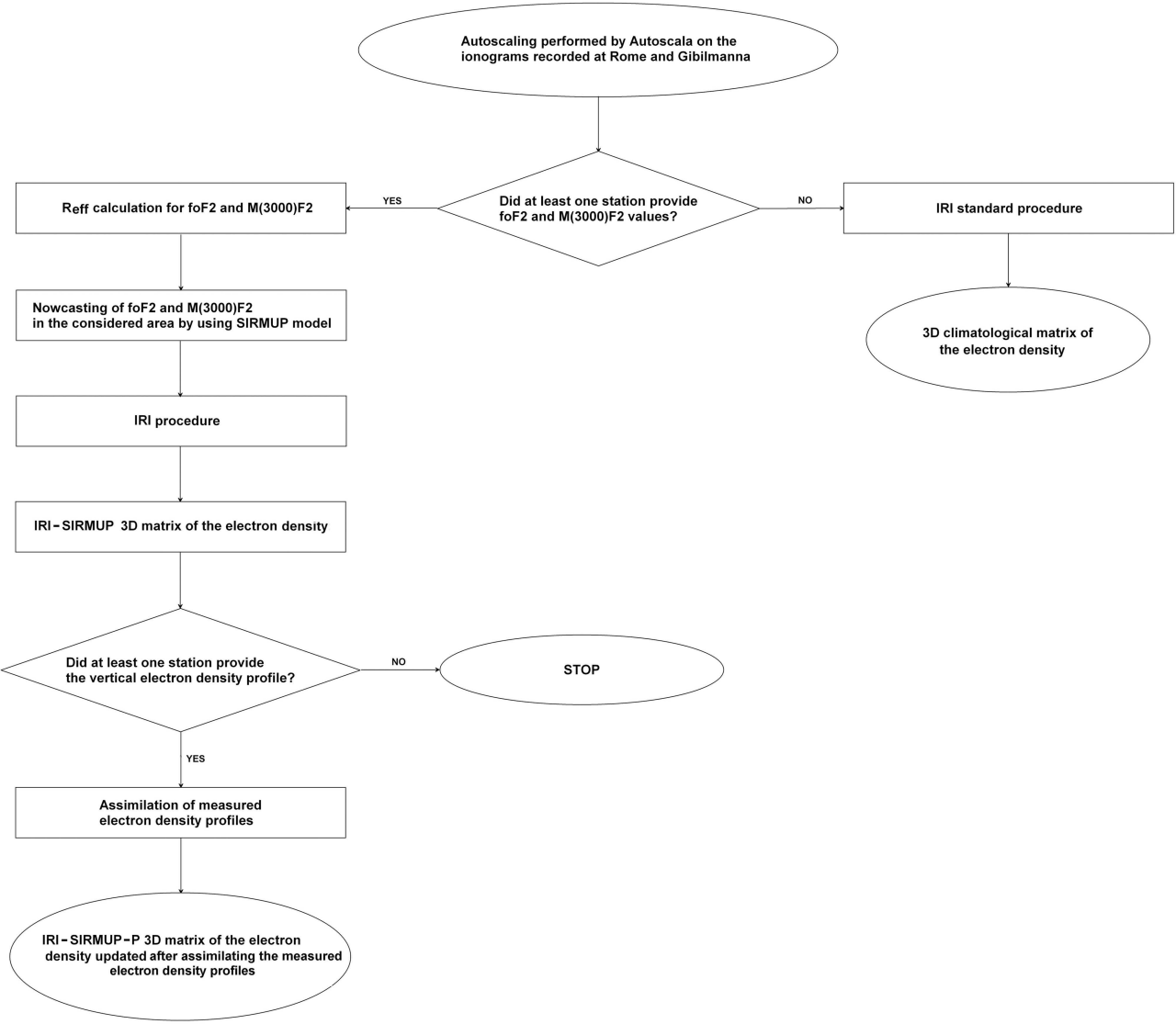
Autoscaling performed by Autoscala on the ionograms recorded at Rome and Gibilmanna
Did at least one station provide foF2 and M(3000)F2 values?
YES
NO
Reff calculation for foF2 and M(3000)F2
IRI standard procedure
Nowcasting of foF2 and M(3000)F2 in the considered area by using SIRMUP model
3D climatological matrix of the electron density
IRI procedure
IRI-SIRMUP 3D matrix of the electron density
Did at least one station provide the vertical electron density profile?
NO
STOP
YES
Assimilation of measured electron density profiles
IRI-SIRMUP-P 3D matrix of the electron density updated after assimilating the measured electron density profiles

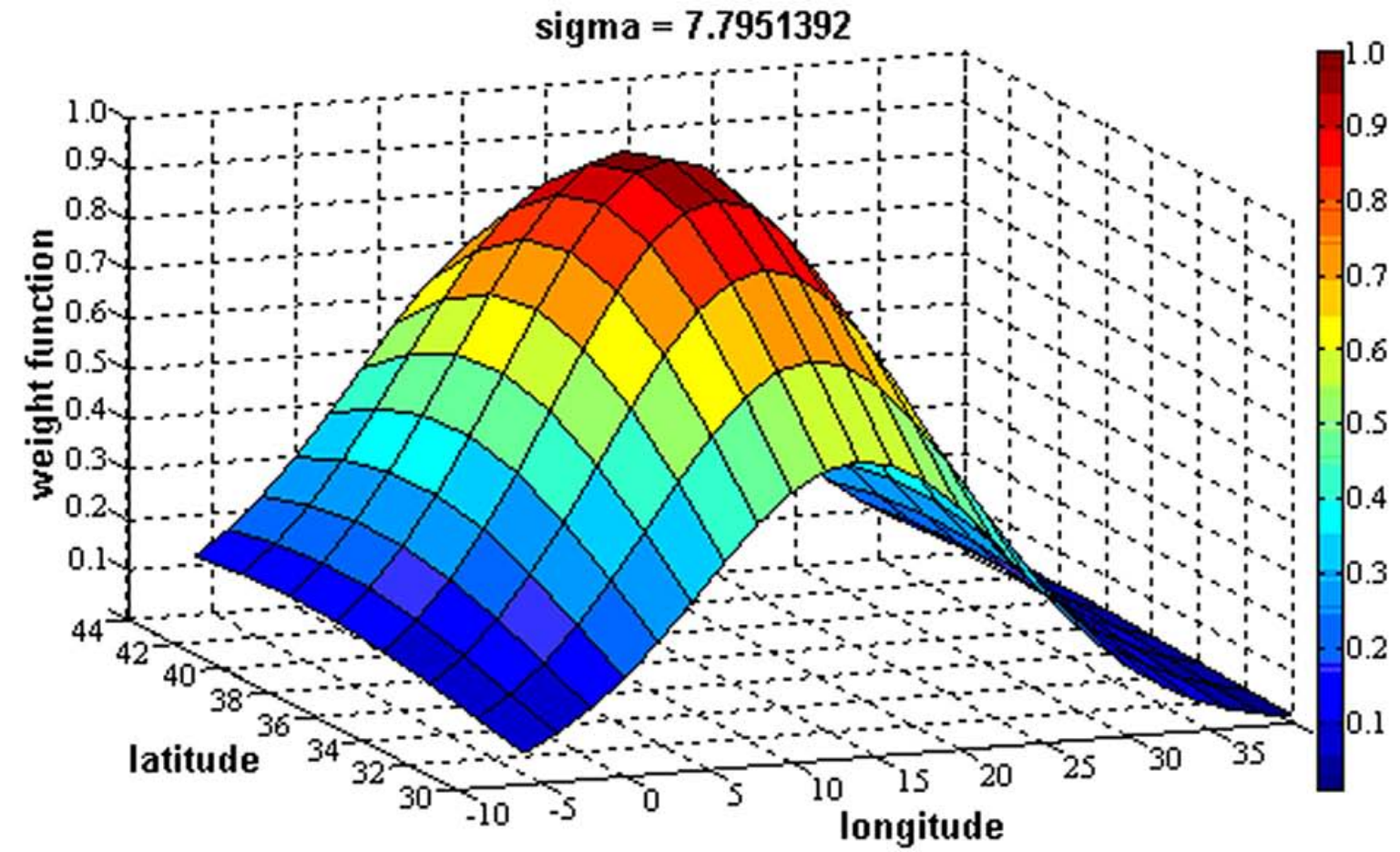
sigma = 7.7951392
weight function
1.0
0.9
0.8
0.7
0.6
0.5
0.4
0.3
0.2
0.1
44
42
40
38
36
34
32
30
latitude
-10
-5
0
5
10
15
20
25
30
35
longitude

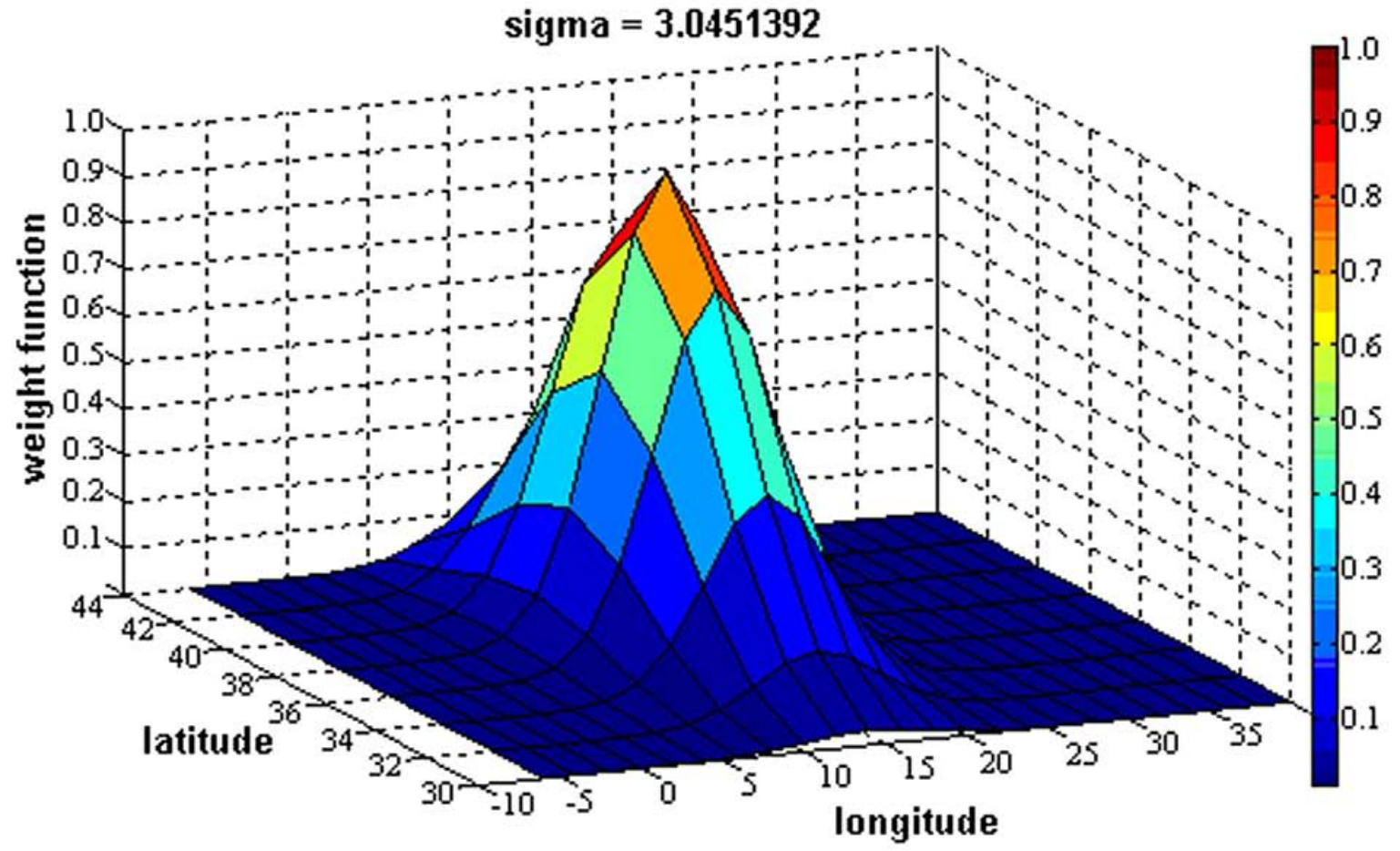
sigma = 3.0451392
weight function
1.0
0.9
0.8
0.7
0.6
0.5
0.4
0.3
0.2
0.1
44
42
40
38
36
34
32
30
latitude
-10
-5
0
5
10
15
20
25
30
35
longitude

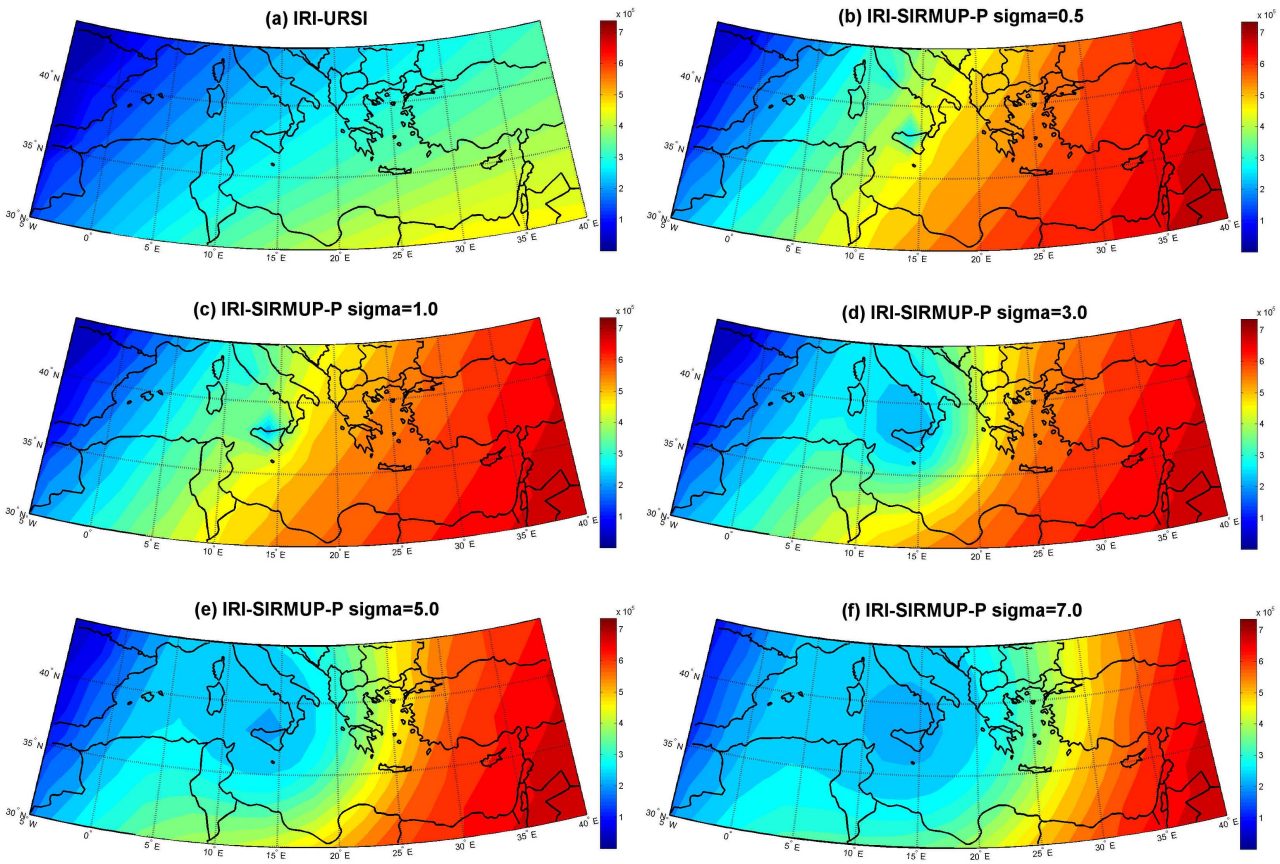
(a) IRI-URSI
(b) IRI-SIRMUP-P sigma=0.5
(c) IRI-SIRMUP-P sigma=1.0
(d) IRI-SIRMUP-P sigma=3.0
(e) IRI-SIRMUP-P sigma=5.0
(f) IRI-SIRMUP-P sigma=7.0
x 10^5
7
6
5
4
3
2
1
40°N
35°N
30°N
5°W
0°
5°E
10°E
15°E
20°E
25°E
30°E
35°E
40°E

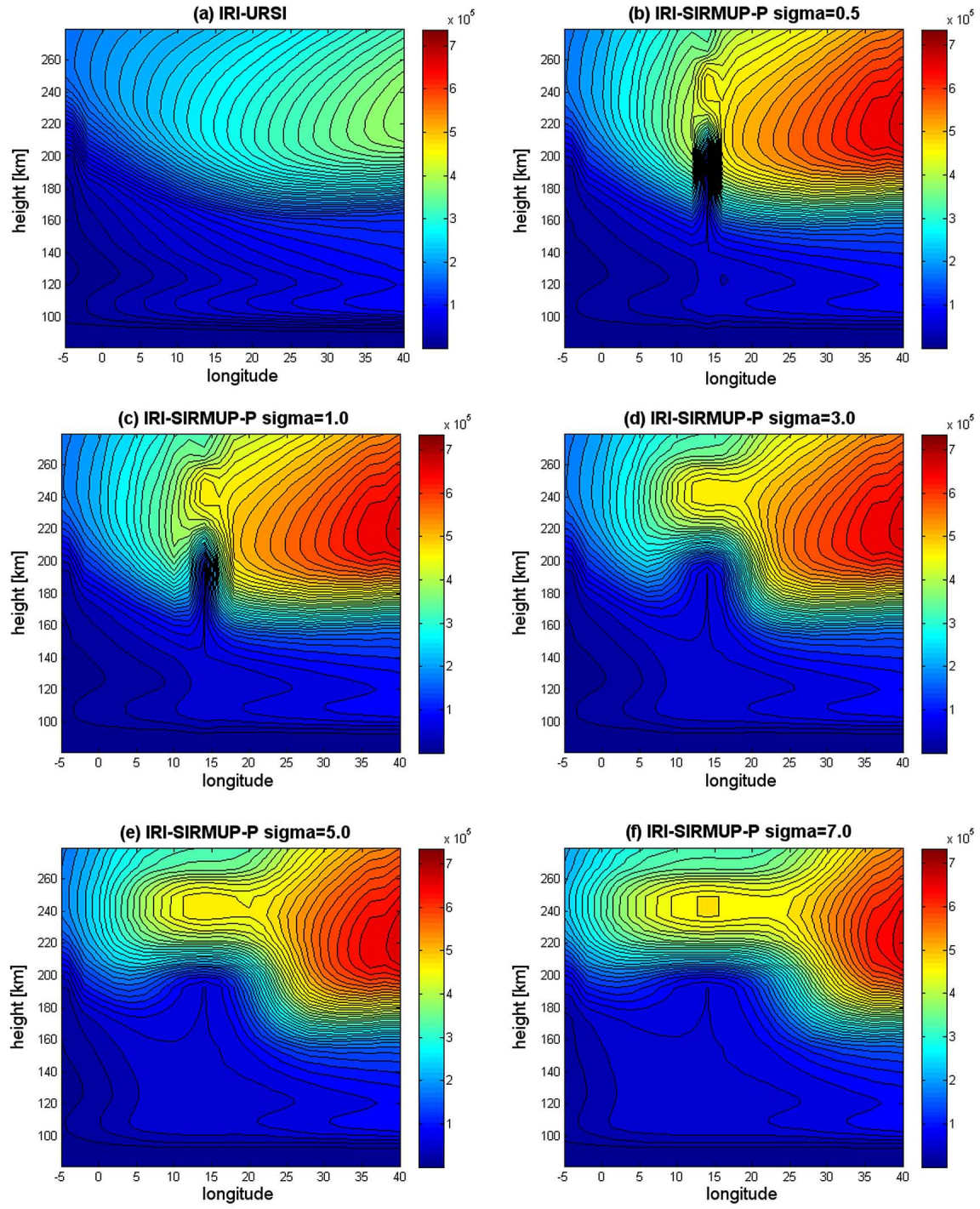
(a) IRI-URSI
(b) IRI-SIRMUP-P sigma=0.5
(c) IRI-SIRMUP-P sigma=1.0
(d) IRI-SIRMUP-P sigma=3.0
(e) IRI-SIRMUP-P sigma=5.0
(f) IRI-SIRMUP-P sigma=7.0
height [km]
longitude
x 10^5

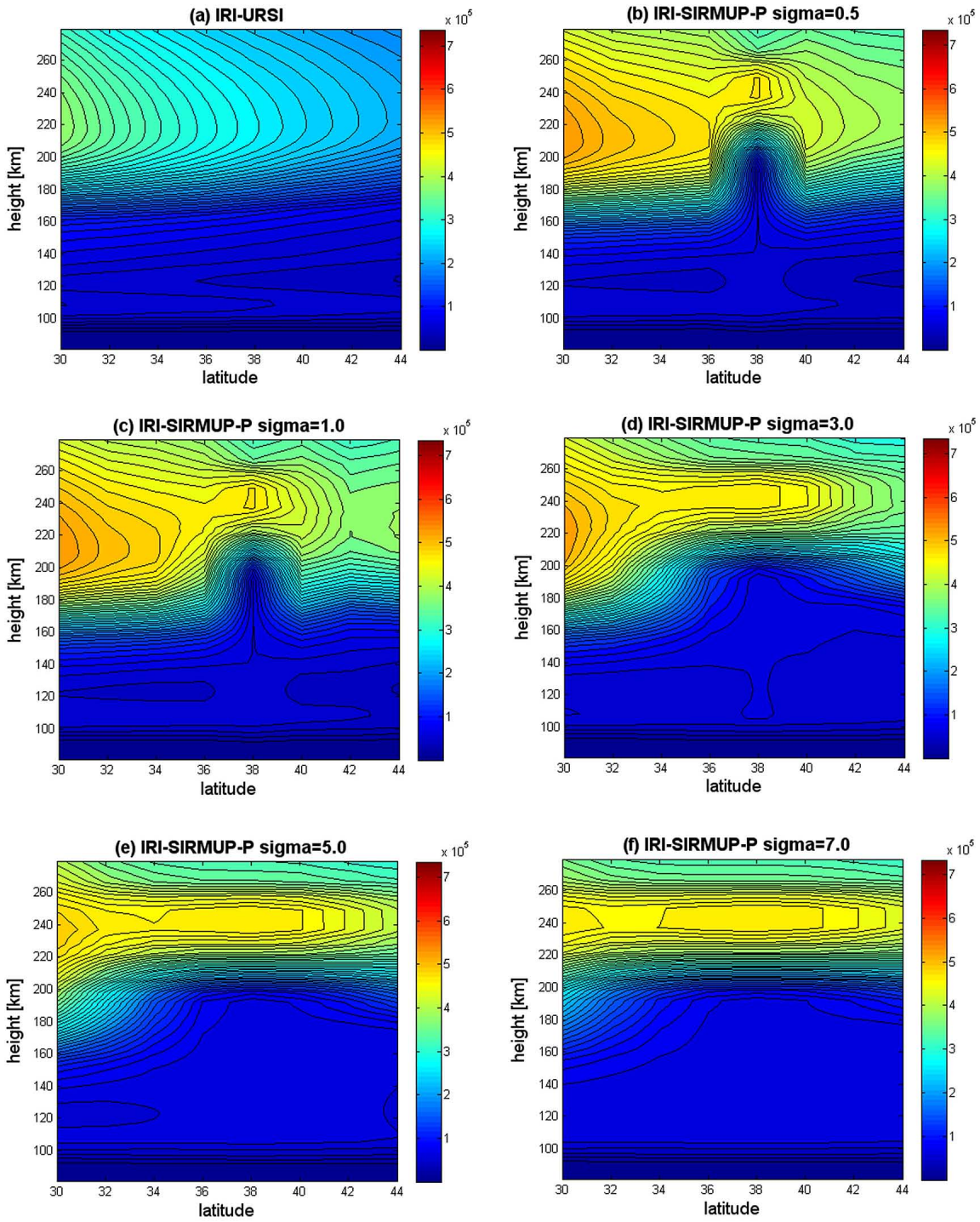
(a) IRI-URSI
(b) IRI-SIRMUP-P sigma=0.5
(c) IRI-SIRMUP-P sigma=1.0
(d) IRI-SIRMUP-P sigma=3.0
(e) IRI-SIRMUP-P sigma=5.0
(f) IRI-SIRMUP-P sigma=7.0
height [km]
latitude
x 10^5

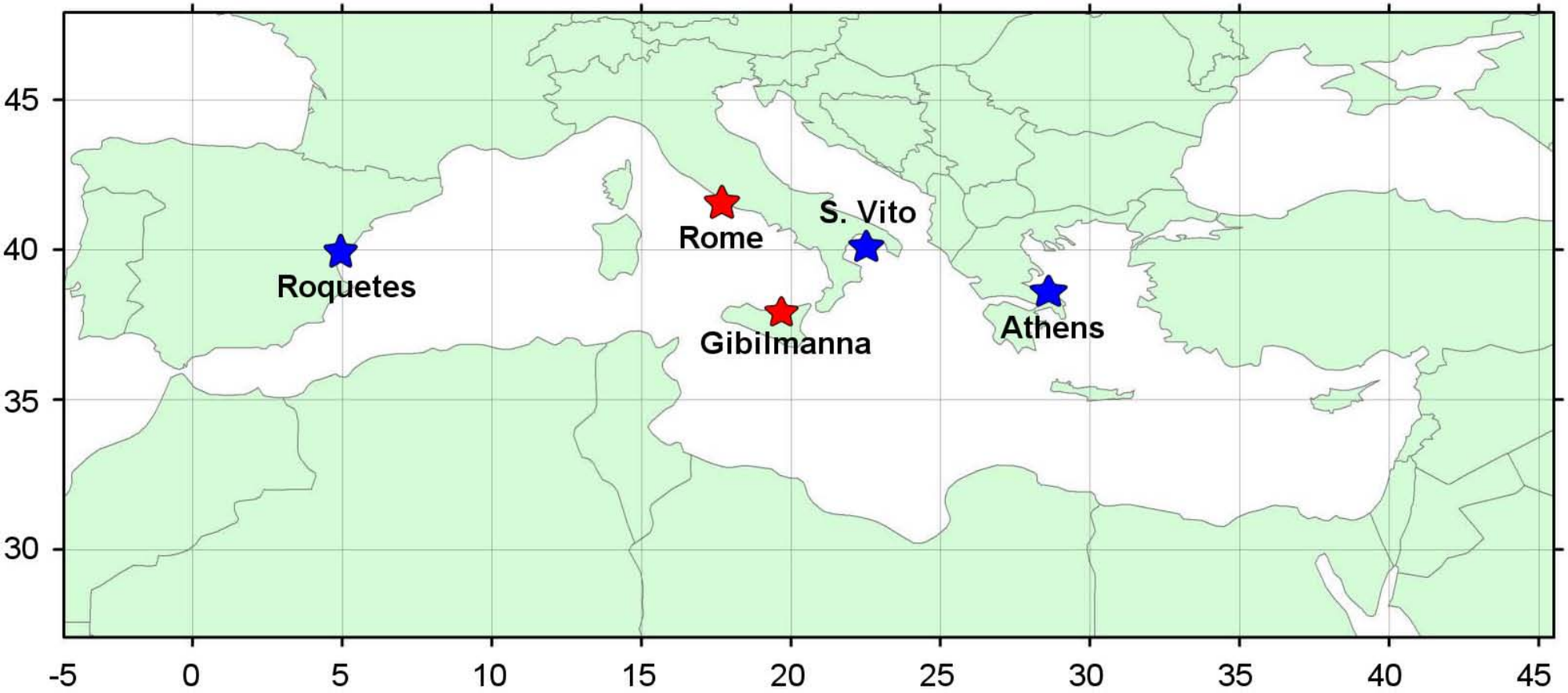
Roquetes
Rome
S. Vito
Gibilmanna
Athens
45
40
35
30
-5
0
5
10
15
20
25
30
35
40
45

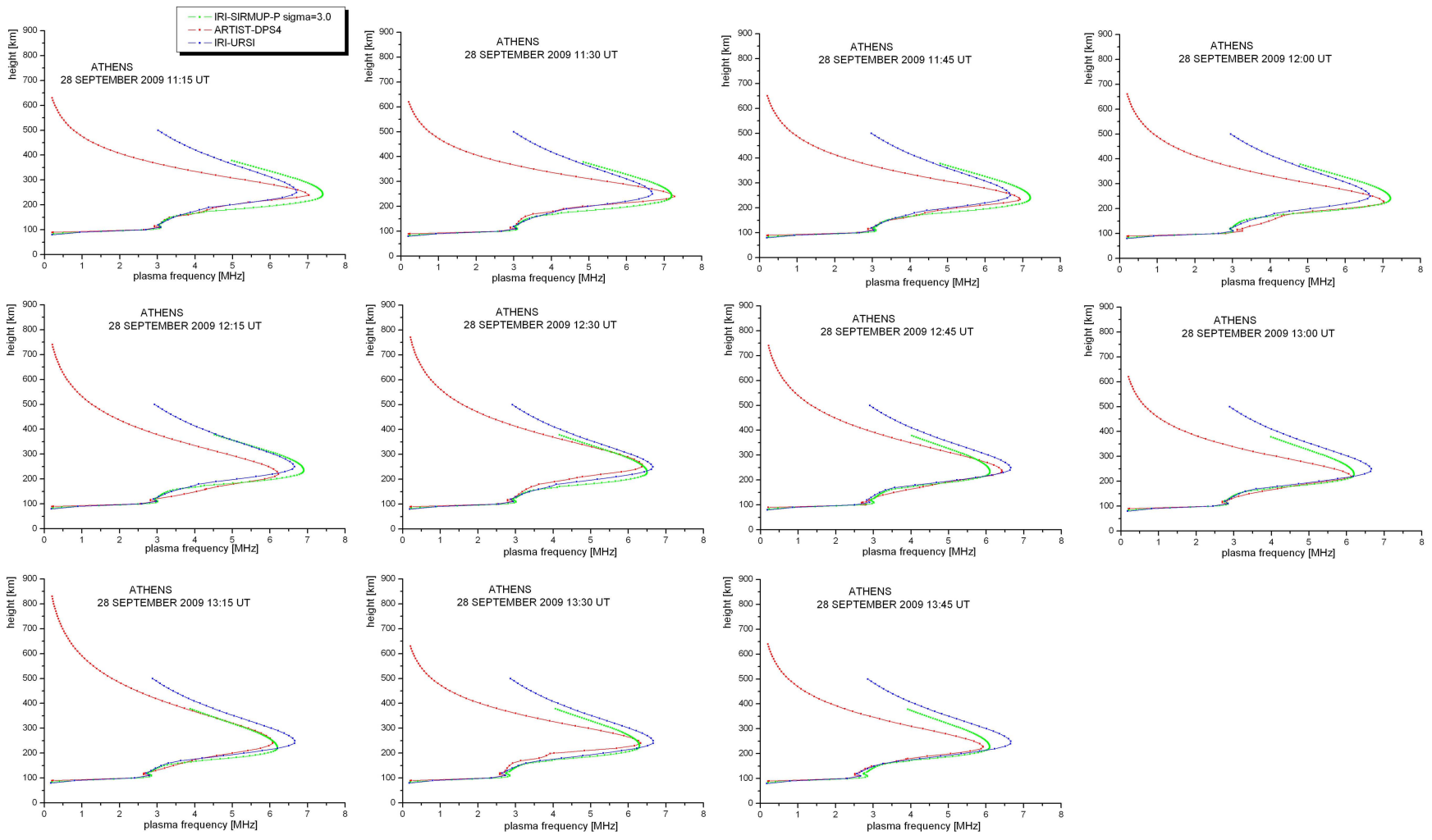
IRI-SIRMUP-P sigma=3.0
ARTIST-DPS4
IRI-URSI
ATHENS
28 SEPTEMBER 2009 11:15 UT
ATHENS
28 SEPTEMBER 2009 11:30 UT
ATHENS
28 SEPTEMBER 2009 11:45 UT
ATHENS
28 SEPTEMBER 2009 12:00 UT
ATHENS
28 SEPTEMBER 2009 12:15 UT
ATHENS
28 SEPTEMBER 2009 12:30 UT
ATHENS
28 SEPTEMBER 2009 12:45 UT
ATHENS
28 SEPTEMBER 2009 13:00 UT
ATHENS
28 SEPTEMBER 2009 13:15 UT
ATHENS
28 SEPTEMBER 2009 13:30 UT
ATHENS
28 SEPTEMBER 2009 13:45 UT
height [km]
plasma frequency [MHz]

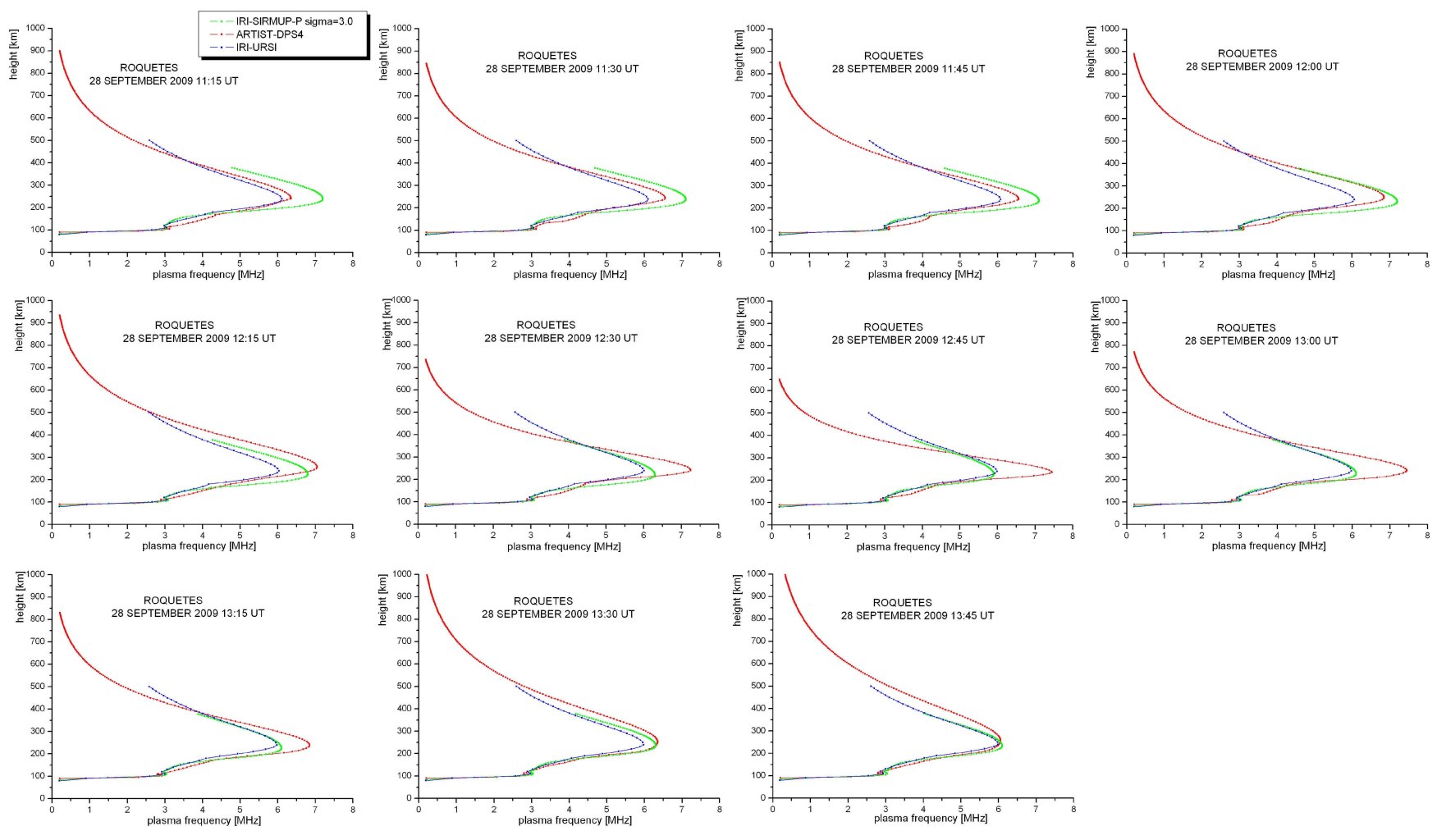
IRI-SIRMUP-P sigma=3.0
ARTIST-DPS4
IRI-URSI
ROQUETES
28 SEPTEMBER 2009 11:15 UT
ROQUETES
28 SEPTEMBER 2009 11:30 UT
ROQUETES
28 SEPTEMBER 2009 11:45 UT
ROQUETES
28 SEPTEMBER 2009 12:00 UT
ROQUETES
28 SEPTEMBER 2009 12:15 UT
ROQUETES
28 SEPTEMBER 2009 12:30 UT
ROQUETES
28 SEPTEMBER 2009 12:45 UT
ROQUETES
28 SEPTEMBER 2009 13:00 UT
ROQUETES
28 SEPTEMBER 2009 13:15 UT
ROQUETES
28 SEPTEMBER 2009 13:30 UT
ROQUETES
28 SEPTEMBER 2009 13:45 UT
height [km]
plasma frequency [MHz]

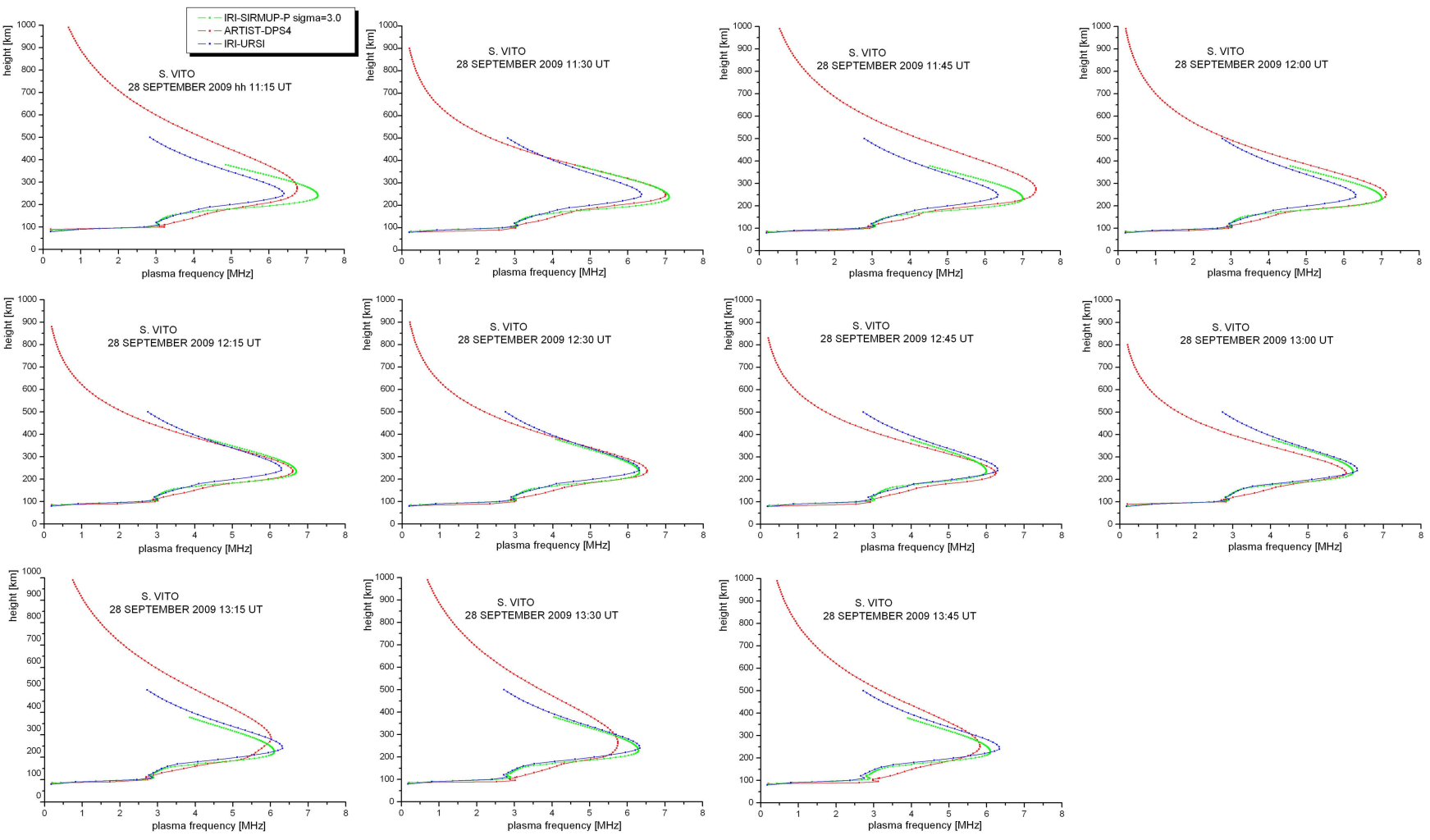
IRI-SIRMUP-P sigma=3.0
ARTIST-DPS4
IRI-URSI
S. VITO
28 SEPTEMBER 2009 hh 11:15 UT
S. VITO
28 SEPTEMBER 2009 11:30 UT
S. VITO
28 SEPTEMBER 2009 11:45 UT
S. VITO
28 SEPTEMBER 2009 12:00 UT
S. VITO
28 SEPTEMBER 2009 12:15 UT
S. VITO
28 SEPTEMBER 2009 12:30 UT
S. VITO
28 SEPTEMBER 2009 12:45 UT
S. VITO
28 SEPTEMBER 2009 13:00 UT
S. VITO
28 SEPTEMBER 2009 13:15 UT
S. VITO
28 SEPTEMBER 2009 13:30 UT
S. VITO
28 SEPTEMBER 2009 13:45 UT
height [km]
plasma frequency [MHz]

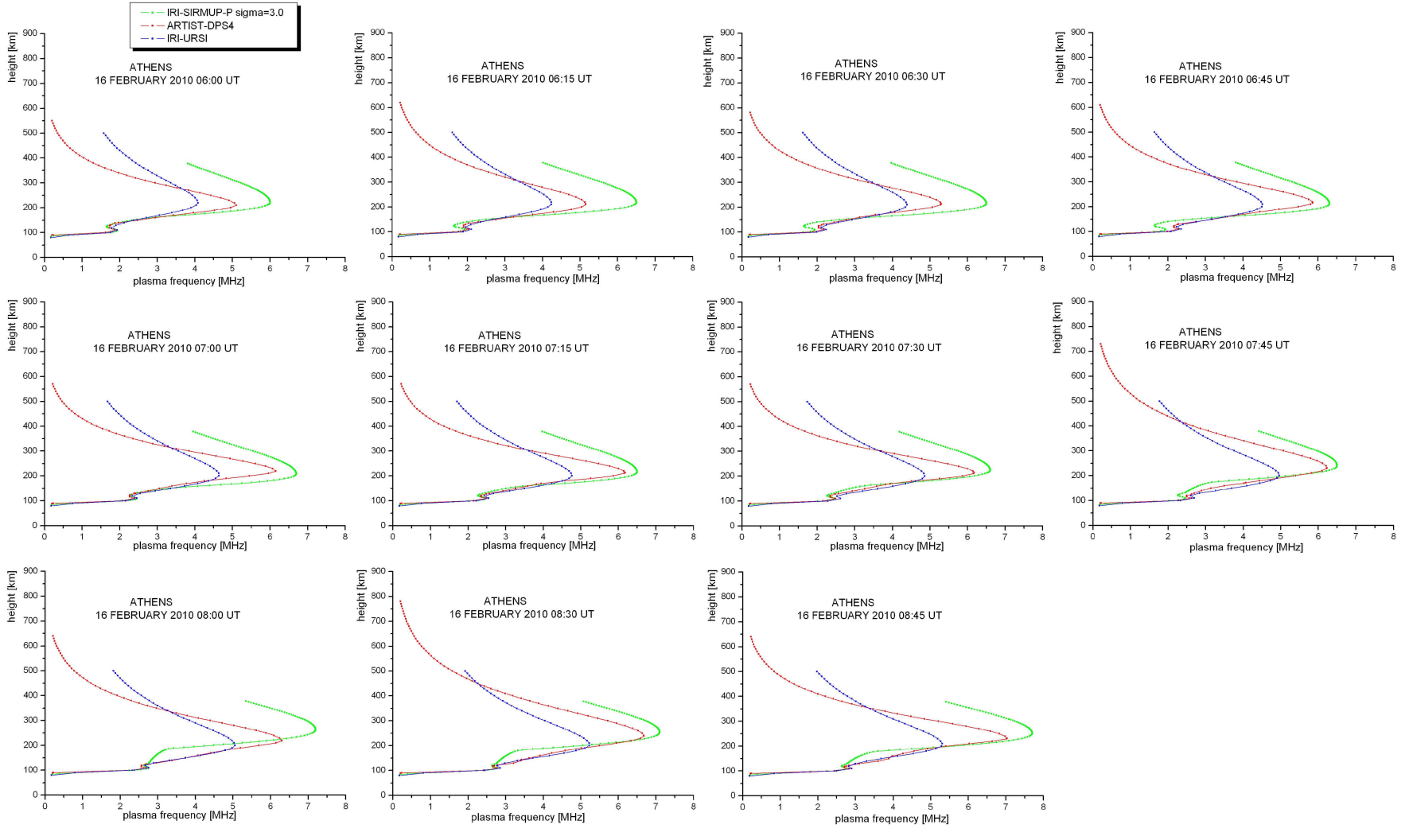
IRI-SIRMUP-P sigma=3.0
ARTIST-DPS4
IRI-URSI
ATHENS
16 FEBRUARY 2010 06:00 UT
ATHENS
16 FEBRUARY 2010 06:15 UT
ATHENS
16 FEBRUARY 2010 06:30 UT
ATHENS
16 FEBRUARY 2010 06:45 UT
ATHENS
16 FEBRUARY 2010 07:00 UT
ATHENS
16 FEBRUARY 2010 07:15 UT
ATHENS
16 FEBRUARY 2010 07:30 UT
ATHENS
16 FEBRUARY 2010 07:45 UT
ATHENS
16 FEBRUARY 2010 08:00 UT
ATHENS
16 FEBRUARY 2010 08:30 UT
ATHENS
16 FEBRUARY 2010 08:45 UT
height [km]
plasma frequency [MHz]

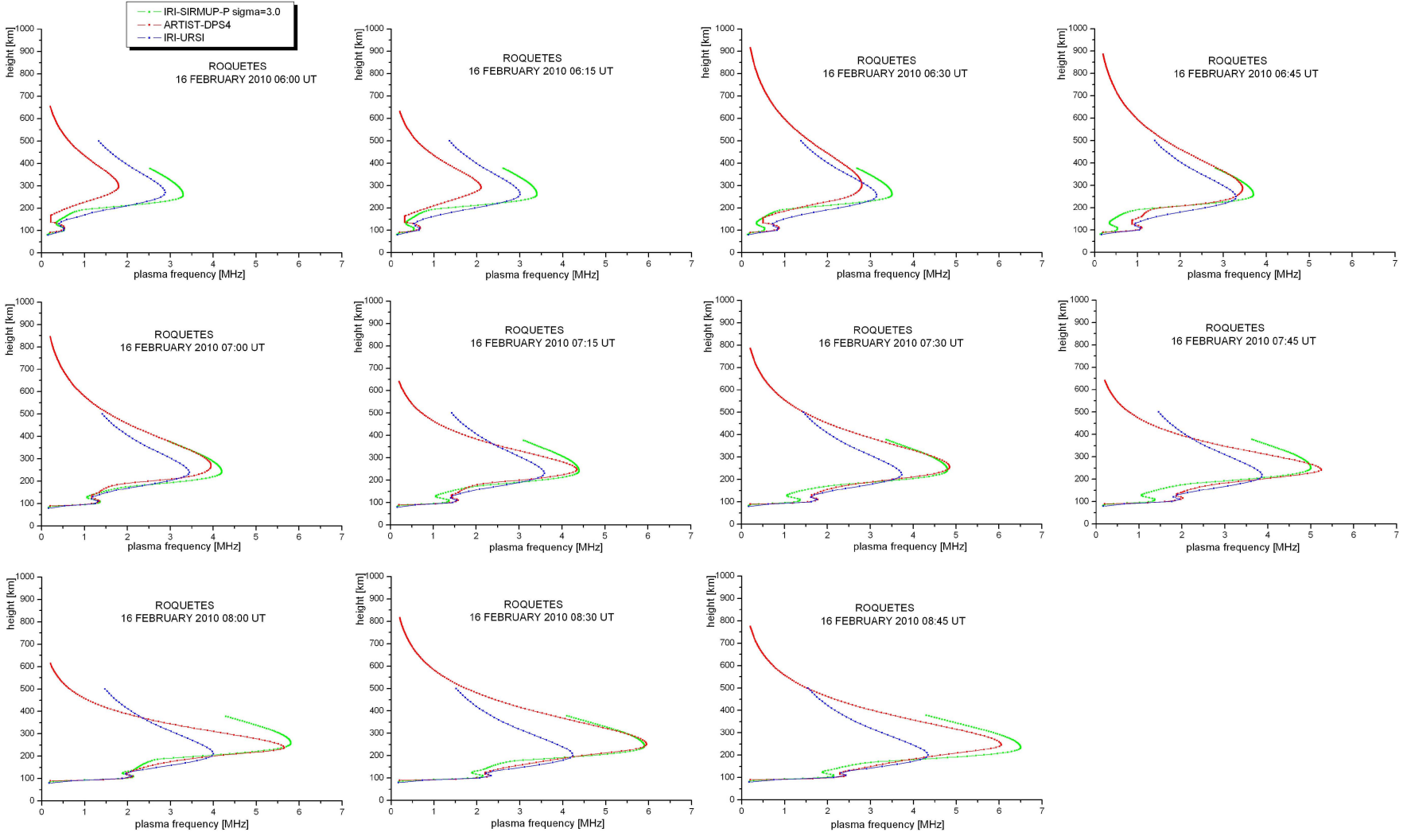
IRI-SIRMUP-P sigma=3.0
ARTIST-DPS4
IRI-URSI
ROQUETES
16 FEBRUARY 2010 06:00 UT
ROQUETES
16 FEBRUARY 2010 06:15 UT
ROQUETES
16 FEBRUARY 2010 06:30 UT
ROQUETES
16 FEBRUARY 2010 06:45 UT
ROQUETES
16 FEBRUARY 2010 07:00 UT
ROQUETES
16 FEBRUARY 2010 07:15 UT
ROQUETES
16 FEBRUARY 2010 07:30 UT
ROQUETES
16 FEBRUARY 2010 07:45 UT
ROQUETES
16 FEBRUARY 2010 08:00 UT
ROQUETES
16 FEBRUARY 2010 08:30 UT
ROQUETES
16 FEBRUARY 2010 08:45 UT
height [km]
plasma frequency [MHz]

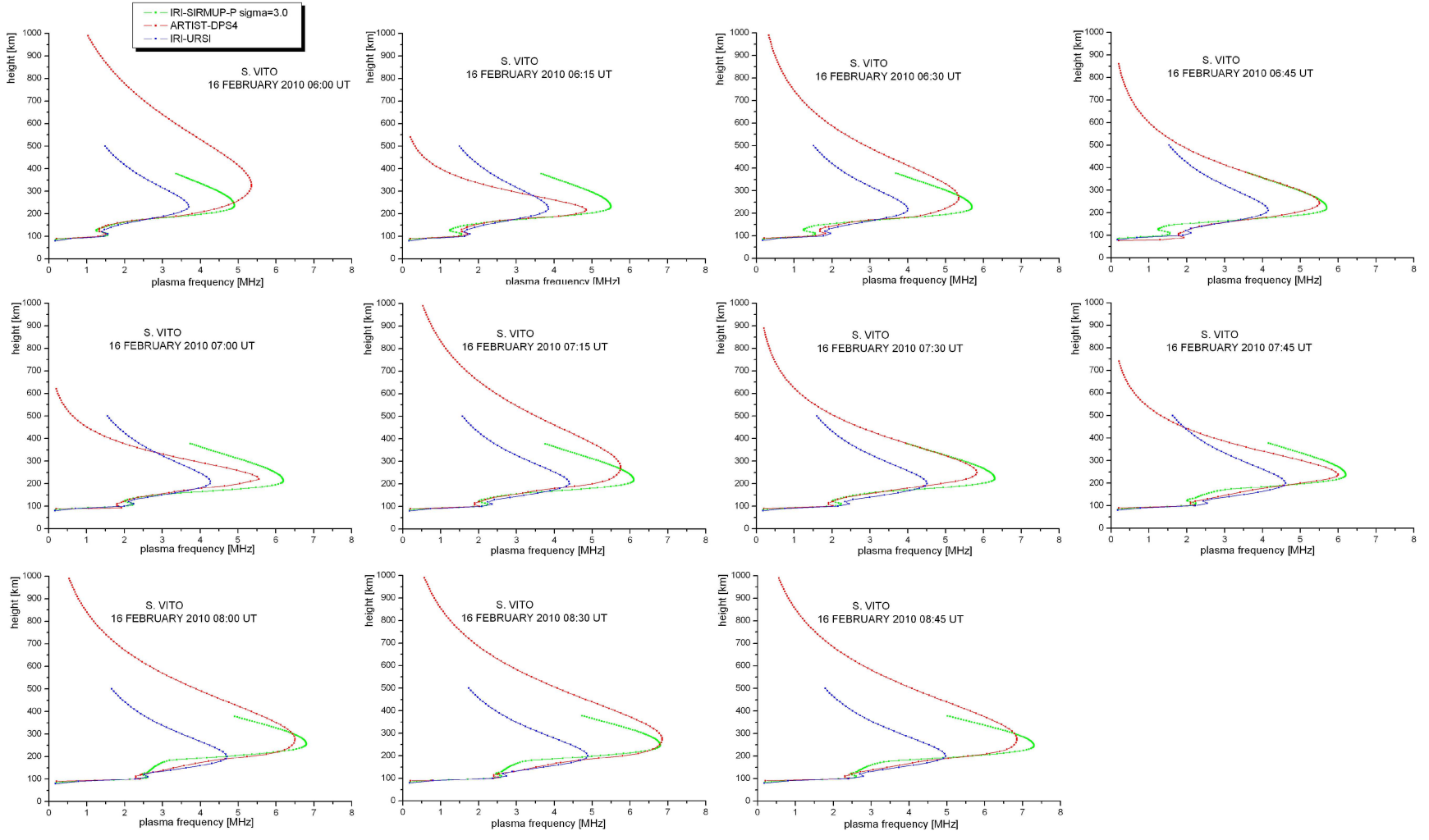
IRI-SIRMUP-P sigma=3.0
ARTIST-DPS4
IRI-URSI
S. VITO
16 FEBRUARY 2010 06:00 UT
S. VITO
16 FEBRUARY 2010 06:15 UT
S. VITO
16 FEBRUARY 2010 06:30 UT
S. VITO
16 FEBRUARY 2010 06:45 UT
S. VITO
16 FEBRUARY 2010 07:00 UT
S. VITO
16 FEBRUARY 2010 07:15 UT
S. VITO
16 FEBRUARY 2010 07:30 UT
S. VITO
16 FEBRUARY 2010 07:45 UT
S. VITO
16 FEBRUARY 2010 08:00 UT
S. VITO
16 FEBRUARY 2010 08:30 UT
S. VITO
16 FEBRUARY 2010 08:45 UT
height [km]
plasma frequency [MHz]

Gibilmanna (lat: +37.9, lon: 014.0) - DATE: 2010 02 16 - TIME (UT): 06:00

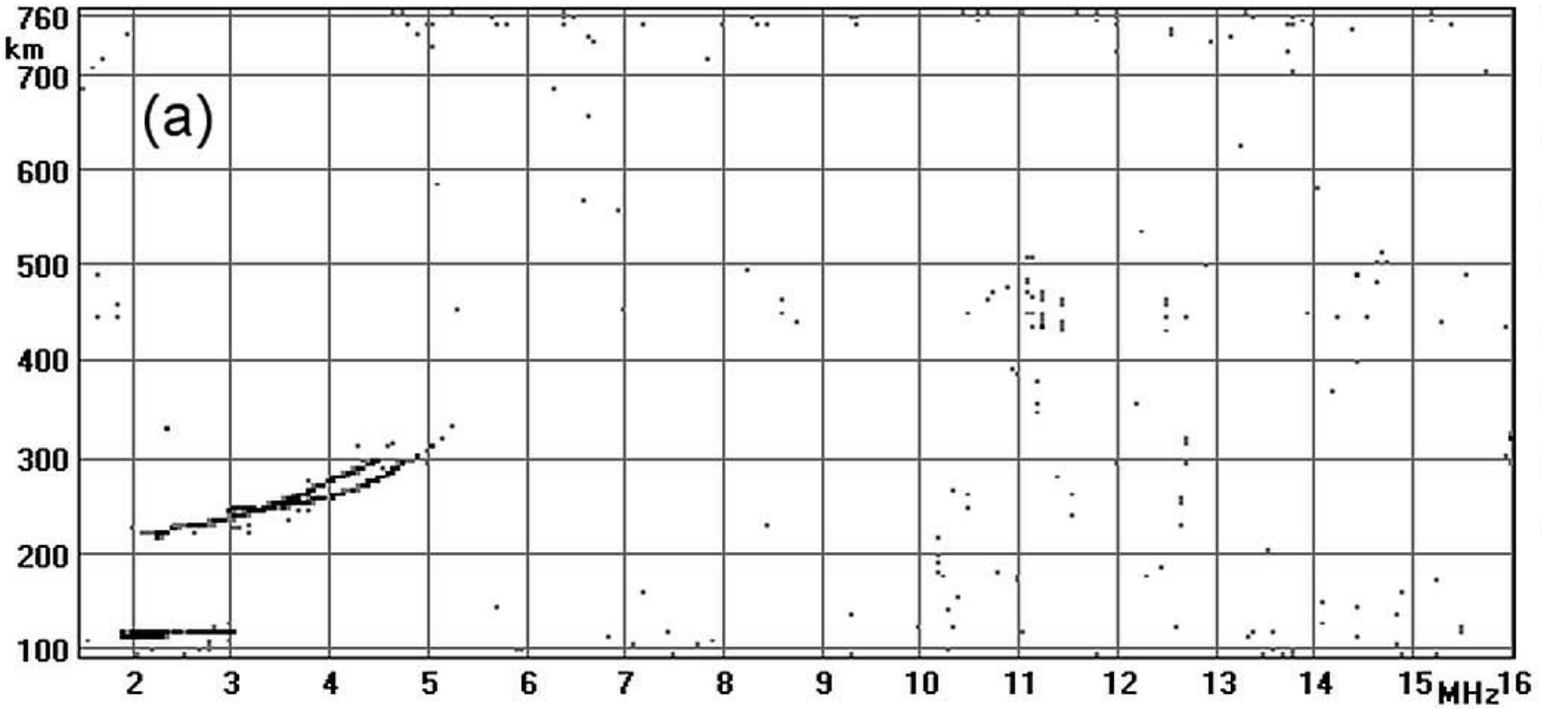

AUTOSCALA output	
foF2	4.9 MHz
MUF(3000)F2	16.6 MHz
M(3000)F2	3.39
fxI	5.6 MHz
foF1	NO
ftEs	3.0 MHz
h'Es	104 km

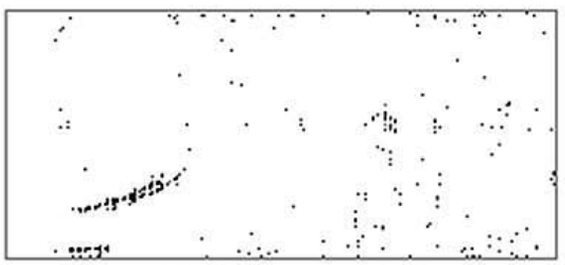

original ionogram resized

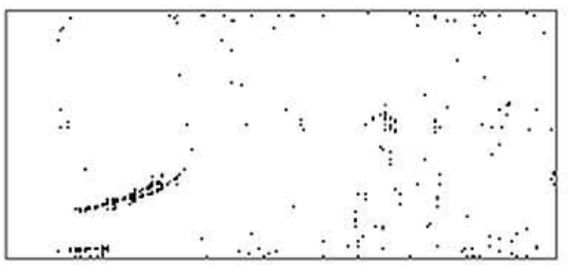

eliminate multiple reflections

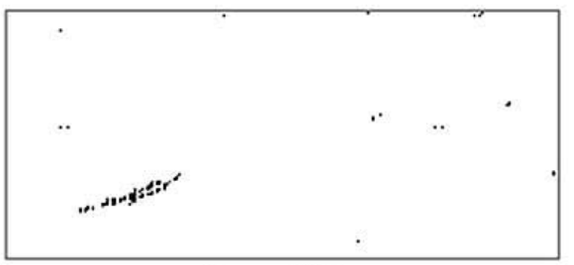

evidence F2 trace

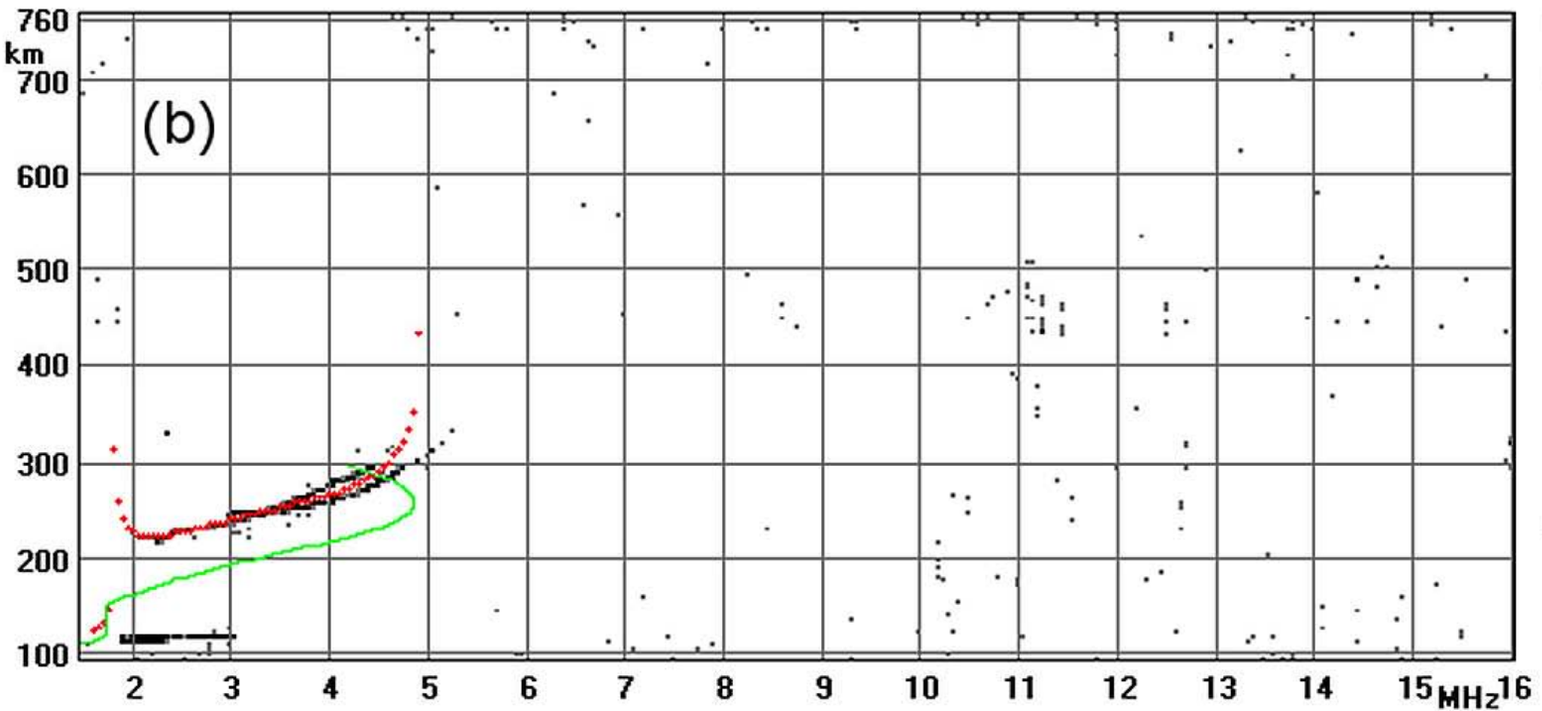

AIP output			
hmF2	247	km	
foF2	04.9	MHz	
foF1	00.0	MHz	[PN]
hmF1	---	km	
D1	00.0		
foE	1.8	MHz	
hmE	110	km	
ymE	20	km	
h_vE	129	km	
Ewidth	30	km	
DelN_vE	00.0	m^(-3)	
B0	074.0	km	
B1	02.5		

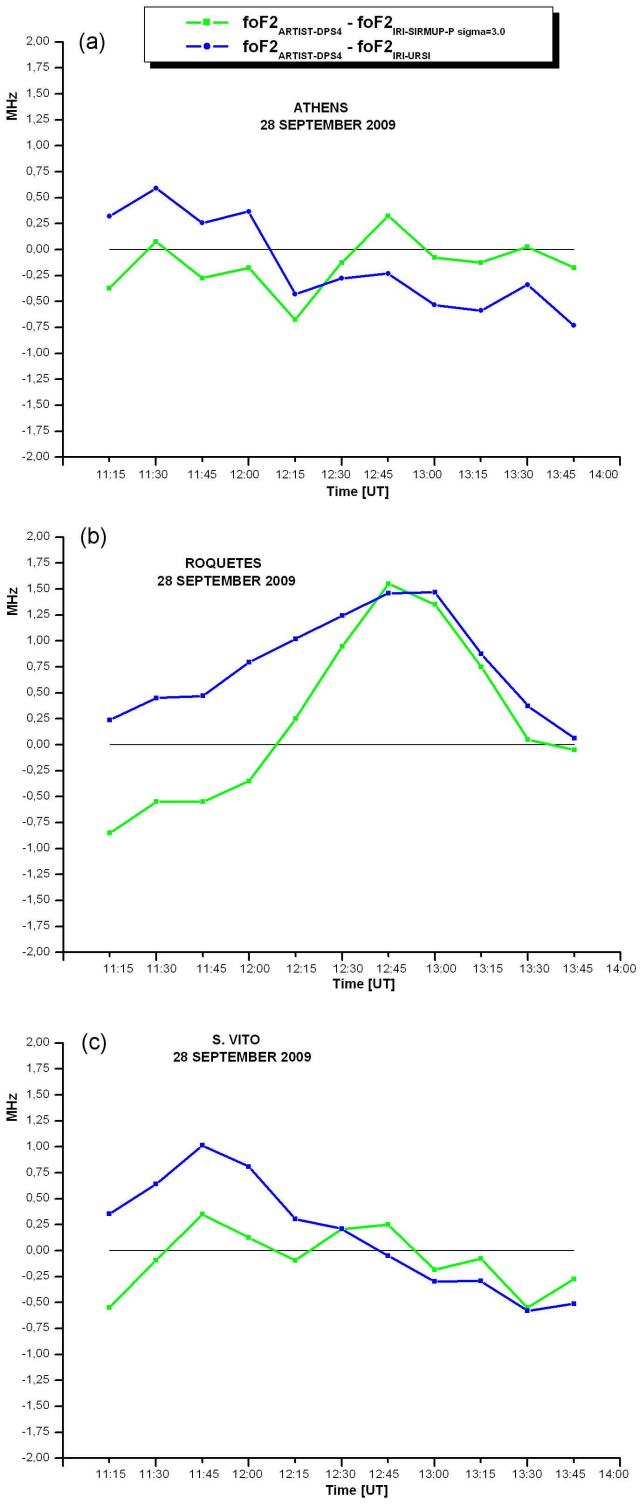
foF2 ARTIST-DPS4 - foF2 IRI-SIRMUP-P sigma=3.0
foF2 ARTIST-DPS4 - foF2 IRI-URSI
(a)
ATHENS
28 SEPTEMBER 2009
MHz
2,00
1,75
1,50
1,25
1,00
0,75
0,50
0,25
0,00
-0,25
-0,50
-0,75
-1,00
-1,25
-1,50
-1,75
-2,00
11:15 11:30 11:45 12:00 12:15 12:30 12:45 13:00 13:15 13:30 13:45 14:00
Time [UT]
(b)
ROQUETES
28 SEPTEMBER 2009
MHz
2,00
1,75
1,50
1,25
1,00
0,75
0,50
0,25
0,00
-0,25
-0,50
-0,75
-1,00
-1,25
-1,50
-1,75
-2,00
11:15 11:30 11:45 12:00 12:15 12:30 12:45 13:00 13:15 13:30 13:45 14:00
Time [UT]
(c)
S. VITO
28 SEPTEMBER 2009
MHz
2,00
1,75
1,50
1,25
1,00
0,75
0,50
0,25
0,00
-0,25
-0,50
-0,75
-1,00
-1,25
-1,50
-1,75
-2,00
11:15 11:30 11:45 12:00 12:15 12:30 12:45 13:00 13:15 13:30 13:45 14:00
Time [UT]

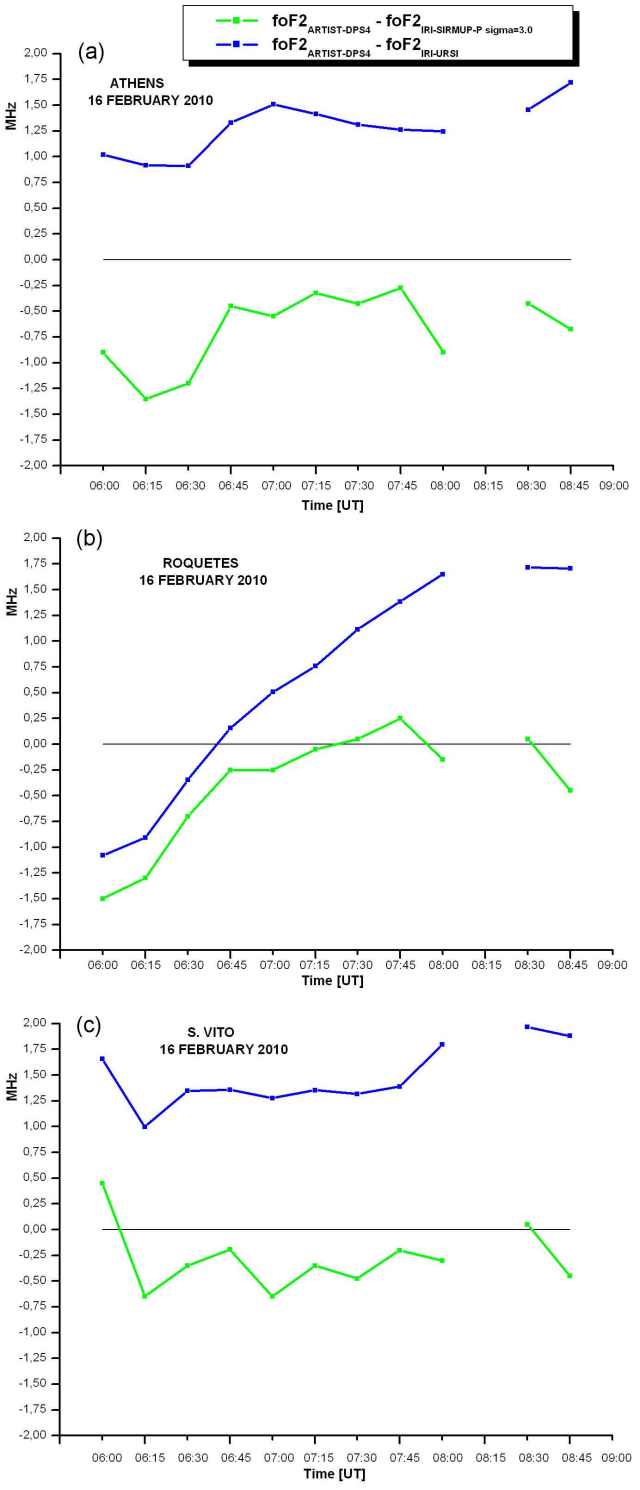
foF2 ARTIST-DPS4 - foF2 IRI-SIRMUP-P sigma=3.0
foF2 ARTIST-DPS4 - foF2 IRI-URSI
(a)
ATHENS
16 FEBRUARY 2010
(b)
ROQUETES
16 FEBRUARY 2010
(c)
S. VITO
16 FEBRUARY 2010
MHz
Time [UT]
06:00 06:15 06:30 06:45 07:00 07:15 07:30 07:45 08:00 08:15 08:30 08:45 09:00